Application of polycarbonate diol containing hindered urea to polyurethane-based clearcoats for tuning of scratch-healing properties

Dong Geun Lee, Sujin Sung, Dae Geun Oh, Young Il Park, Sang-Ho Lee, Jin Chul Kim, Seung Man Noh, Hyun Wook Jung

Abstract Newly synthesized polycarbonate diols containing hindered urea (PCD-HUs) were employed to modify the scratch-healing properties of conventional two-component clearcoats. To elucidate their contributions to the crosslinking properties of the coatings under conventional thermal curing (150°C), the real-time rheological properties of the clearcoat mixtures were measured using a rotational rheometer in the small-amplitude oscillatory shear mode. A dynamic mechanical analysis was carried out to compare the thermomechanical properties of the cured clearcoat free films. PCD-HU, a key component for the tuning of the scratch-healing, was further identified by analyzing the clearcoat layer cured over a phosphated metal substrate with undercoats such as primer and basecoat as a precoated metal (PCM) sheet. Elastic recovery and scratch profiles of the outermost clearcoat layer in the PCM sheet were acquired through nano-indentation and nano-scratch tests by gradually increasing the quantitative normal force. Finally, the healing patterns of the scratches on various clearcoat layers at a certain normal force were visualized by three-dimensional and one-dimensional cross-cut images using atomic force microscopy under specified temperature and healing time conditions. The surface durability provided by the PCD-HU in the clearcoat layer was confirmed by repeated scratching and healing tests on the same surface positions. Therefore, the coating layer containing HU, which possessed similar surface mechanical properties to those of conventional references, exhibited better scratch-healing performance.

Keywords Polyurethane-based clearcoat, Polycarbonate diol with hindered urea, Real-time rheological properties, Nano-scratch test, Scratch-healing

Dong Geun Lee and Sujin Sung have contributed equally to this study.

D. G. Lee, D. G. Oh, H. W. Jung (✉)
Department of Chemical and Biological Engineering, Korea University, Seoul 02841, Republic of Korea
e-mail: hwjung@grtrkr.korea.ac.kr

S. Sung, Y. I. Park, S.-H. Lee, J. C. Kim (✉),
S. M. Noh (✉)
Research Center for Green Fine Chemicals, Korea Research Institute of Chemical Technology, Ulsan 44412, Republic of Korea
e-mail: jckim81@krict.re.kr

S. M. Noh
e-mail: smnoh@krict.re.kr

D. G. Oh
Research and Development Center, Noroo Bee Chemical Cooperation, Cheonan 31094, Republic of Korea

Introduction

The clearcoat, the outermost layer in automotive coatings, is inevitably exposed to various external harmful stress conditions. The clearcoat generally has two functions. The first is to protect the undercoats (primer, basecoat, and e-coat) and car body from external detrimental factors such as acid rain, stone chips, bird droppings, and marring. A high surface hardness is required for this functionality. By regulating the crosslink density[1,2] or introducing nanoparticles or nano-fillers,[3–7] several studies have been performed to improve the hardness of the clearcoat with respect to external stresses. The clearcoat layer actually consisted of various organic–inorganic hybrid ingredients, in contrast to the undercoat layers.[8] The second main function of the clearcoat is to sustainably display aesthetic colors with a high gloss. To effectively reflect this function, a material composition and curing

conditions that are suited to the specified application are required. As the appearance of the cured coating surface is directly related to the gloss, the scratch-healing property is the crucial factor to retain the high-gloss feature. Considering the above functionalities, the clearcoat layer should guarantee a high hardness and good scratch-healing feature against external mechanical stresses and chemicals. However, these requirements lead to a trade-off relationship and thus should be properly compensated according to the application.

The properties can be adequately balanced by introducing two-component (2 K) polyurethane (PUR) coatings, exhibiting good abrasion resistance, increased hardness, good flexibility, and high resistance to chemicals and solvents,[9,10] which have been widely used in the automotive coating processes. The urethane reaction between the hydroxyl functional group of a polyol resin and isocyanate group of a crosslinker forms densely crosslinked networks under normal heating conditions (120–150°C for 30 min). The 2 K PUR coatings could be easily modified by changing the chemical structure and composition of the main polyol resin and/or isocyanate crosslinker, depending on the target application. In general, a higher ratio of the aliphatic group in the polyol resin and crosslinker provides a more flexible polymer network. On the contrary, a higher portion of the cyclic or aromatic group leads to more rigid crosslinked networks. The proper ratio of aliphatic or aromatic groups should be determined for the balanced flexible and hard characteristics of the clearcoat layer.

A methodology to remedy scratches in the PUR clearcoat layer at ambient temperature has been developed. Reversible intrinsic-bondage-based materials could be inserted in clearcoat systems to achieve scratch-healing. This technique seems to be advantageous over the extrinsic methods, which typically involve a one-time healing material capsule, refillable capillary, or hollow channel,[11] since it can be applied to multiple healing treatments in contrast to the one-time method. Various studies have been carried out to heal cracked or scratched polymeric layers using chemical or physical bond-based methods such as disulfide bonding,[12–14] hydrogen bonding,[15,16] and Diels–Alder reaction.[17] Despite their features, these methods still cannot be directly applied to hard coating types including the clearcoat, owing to the restriction to coatings with relatively low moduli. Therefore, advanced techniques should be further developed to realize the healing mechanism in more highly crosslinked clearcoat layers. Recently, several studies have dealt with intrinsic self-healing methods, employing the Diels–Alder reaction[18,19] and hindered urea[20] (HU) for applying to highly dense coatings. The HU group has been recently introduced by Ying et al.[21] The advantage of the coating system containing HU is the reversible attachment and detachment of the urea

group even under catalyst-free and ambient room-temperature conditions, whereas the Diels–Alder bonds require a relatively high temperature over 130°C for their reversibility. Therefore, in this study, we focus on the newly synthesized polycarbonate diol (PCD) with the HU group combined with conventional clearcoat resin to improve the repeated scratch-healing characteristics of the clearcoat systems.

To analyze the scratch-healing behaviors of the clearcoats in detail, it is essential to acquire reliable quantitative scratches and actual profiles of fractured surfaces on cured films. Micro- or nano-scratch tests would be more appropriate for this purpose than their alternatives.[22–24] The best results could be achieved if visualization techniques are introduced to correctly observe the accurate scratch transition. Noh et al.[25,26] reported the effects of blocked polyisocyanate crosslinkers in automotive clearcoats on scratch characteristics based on three-dimensional (3D) scratch profiles using atomic force microscopy (AFM). Kutschera et al.[27] correlated the scratch resistances and structural factors of clearcoat samples produced through various curing modes [i.e., thermal, ultraviolet (UV), and dual-curing] using an AMTEC car wash simulator and AFM. The detailed observation of the healing process under specified temperature conditions can finely reveal the scratch-healing dynamics of the clearcoat layer during the time evolution.[28–30]

In this study, we synthesized polycarbonate diols containing the hindered urea group (PCD-HUs) with tunable flexibility to enhance the scratch-healing performance of the clearcoat layer. The synthesized polyols were mixed with conventional clearcoat resins and thermal crosslinker to fabricate thermally cured coatings and form a polyacrylate-graft-poly(carbonate urea urethane) network. The real-time curing behaviors of the reactive clearcoat mixtures were analyzed using the small-amplitude oscillatory shear (SAOS) mode of a rotational rheometer. The thermomechanical properties of the cured free films were measured using a dynamic mechanical analysis (DMA). The clearcoat mixtures were deposited and cured over precoated metal (PCM) sheets with primer and basecoat sub-layers to evaluate the elastic recovery and scratch characteristics of the realistic automotive coating layers using nano-indentation and nano-scratch testers (NST). In particular, the NST could offer reliable scratch patterns on the coating surface corresponding to the specific normal force. The temporal scratch patterns under various temperatures and durations were envisioned by AFM. In addition, scratching and thermally driven healing procedures were repeated several times to evaluate the durability of the coating surface against repetitive external stresses applied at the same positions. Therefore, the real-time curing behaviors and film scratch-healing properties of the clearcoats containing the newly synthesized PCD-HUs were correlated for possible clearcoat applications.

Experimental methods

Preparation of PCD-HUs

Synthesis

Hexamethylene diisocyanate (HDI), isophorone diisocyanate (IPDI), dibutyltin dilaurate (DBTDL), *N*,*N*′-di-*tert*-butylethylenediamine, and 2-butanone were purchased from Sigma-Aldrich and used as received. An acryl polyol binder, HDI trimer (Desmodur® N3300A), and PCD (DURANOL™ T5650J, $\overline{M}_n$ = 800, OH value = 130–150) were supplied from Noroo Bee Chemicals and Asahi Kasei Corporation. The synthesis starting from the diisocyanate monomers (HUI-DI and HUH-DI) to obtain PCD-HUs (PCD-HUI and PCD-HUH) is illustrated in Fig. 1. To synthesize the HU diisocyanates based on the IPDI structure (HUI-DI) (Fig. 1a), an *N*,*N*′-di-tert-butyl ethylene diamine (3.00 g, 17.4 mmol) solution in 2-butanone (20 mL) was slowly added into an IPDI (7.74 g, 34.8 mmol) solution in 2-butanone (10 mL) through a dropping funnel under stirring for 2 h at 35°C. The HUI-DI solution was mixed into a PCD solution in 2-butanone (27.8 g of PCD and catalytic amount of DBTDL in 50 mL of 2-butanone) under stirring at 70°C for 1 h and subsequently at 150°C for 30 min to obtain PCD-HU based on the IPDI structure (PCD-HUI, Fig. 1b). After the completion of the urethane reaction between HUI-DI and PCD, the reaction mixture was concentrated using a rotary evaporator under a reduced pressure. Finally, PCD-HUI was obtained in the form of a colorless viscous liquid with quantitative yield. The synthesis of the PCD-HU based on the HDI structure (PCD-HUH) was generally identical to that for PCD-HUI, except that HDI was used instead of IPDI.

Fourier-transform infrared (FTIR) analysis

FTIR spectra of HUI-DI, HUH-DI, PCD-HUI, and PCD-HUH were recorded in the region of 4000–500 cm^{-1} using a FTIR spectrometer (Nicolet 6700/Nicolet Continuum FTIR spectrometer, Thermo Fisher Scientific Inc., USA) in the transmittance mode under ambient conditions. The urethane reactions between the PCD and diisocyanates (HUI-DI and HUH-DI) with the HU group, yielding PCD-HUI and PCD-HUH, respectively, were confirmed by the disappearance of the isocyanate unit (–NCO) band at 2250 cm^{-1} observed for HUI and HUH, and by the intensity of the methylene unit (–CH$_2$–) band at 2950–2850 cm^{-1} (Fig. 2).

Molecular weights

The number-average and weight-average molecular weights ($\overline{M}_n$, $\overline{M}_w$) and molecular weight distributions
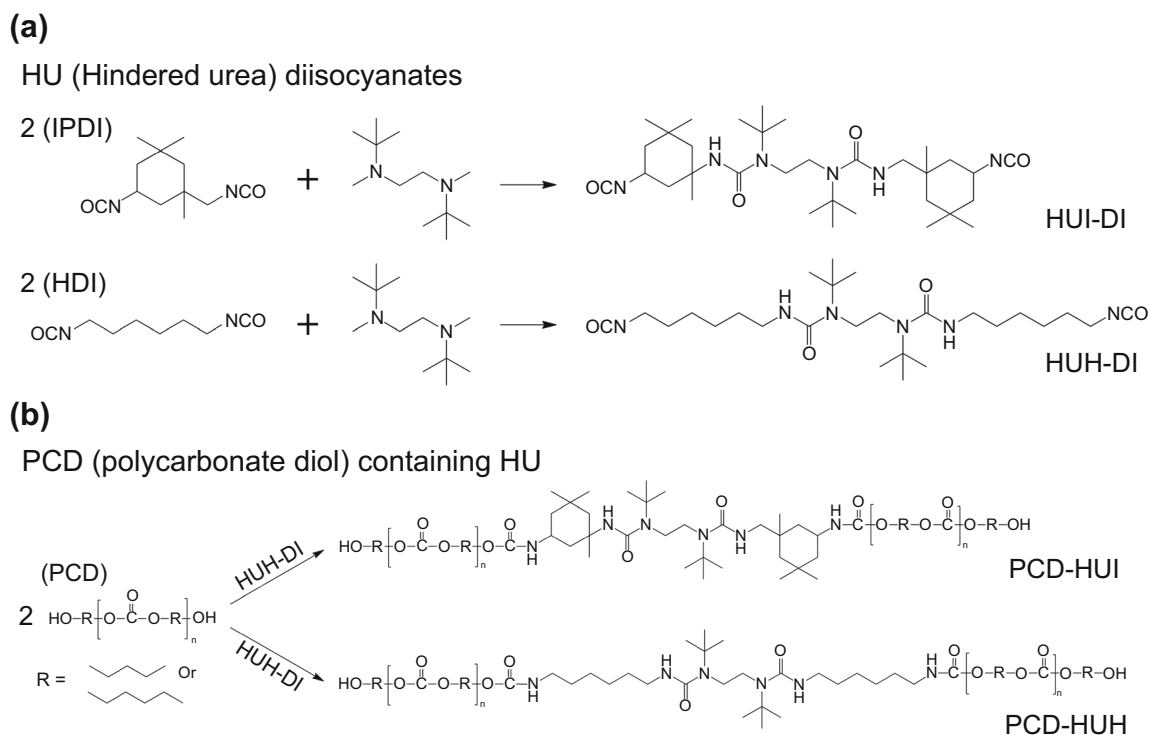

Fig. 1: Synthesis procedures of (a) hindered urea containing diisocyanates (HUI-DI and HUH-DI) and (b) polycarbonate diol containing HU (PCD-HUI and PCD-HUH)

(D_M) of the synthesized PCD-HUI and PCD-HUH were determined using a size-exclusion chromatography apparatus (SEC Agilent Tech 1260, Agilent, USA) equipped with a set of gel columns (Agilent PLgel 5 μm MIXED-D column). The system was equilibrated at 25°C in anhydrous tetrahydrofuran, which was used as the polymer solvent and eluent with a flow rate of 1 mL min^{-1}, and calibrated with polystyrene standards ($\overline{M}_w$: 650–6,375,000). Their properties including their OH values are presented in Table 1.

Fig. 2: FTIR spectra of (a) IPDI, HUI-DI, and PCD-HUI and (b) HDI, HUH-DI, and PCD-HUH

Preparation of clearcoat coatings and their property measurements

Reference clearcoats

Commercial 2 K clearcoats produced by Noroo Bee Chemical (Cheonan, Korea) were selected as the reference samples in this study. The resin mainly consisted of acryl polyol or PCD. The acryl polyol with an OH value of 95–100 ($\overline{M}_w = 10,000$–20,000, $T_g = 50°$ C) was originally designed by Noroo Bee Chemical. T50 denotes the clearcoat sample having only acryl polyol resin, while T30 is the clearcoat consisting of mixed resins with acryl polyol and PCD in a weight ratio of 3:1. Their formulations are presented in Table 2. Swasol 1500 (Maruzen Chemical, Japan), xylene, and butyl acetate were used as solvents. To improve the light resistance of the clearcoat, UV absorber and light stabilizer were added and the DBTDL catalyst was used to accelerate the curing reaction. The final OH values of T50 and T30 were 64.7 and 69.0 mg KOH/g, respectively. The HDI trimer (NCO content = 22–24%) was supplied from Asahi Kasei Corporation and used as a thermal crosslinker to cure the coating film.

Clearcoat mixtures containing PCD-HUs

The synthesized PCD-HUI and PCD-HUH polyols with the same nonvolatile values as references were mixed with T50 to obtain possible clearcoats (10 and 30 wt% of T50, see Table 3). The sample names defined to distinguish the coatings are presented in Table 3. For example, the coating sample having a PCD-HUI content of 10 wt% (with respect to T50) is denoted as HI-10. The mixing between the main resin and crosslinker was carried out under equivalent amounts of NCO (in crosslinker) and OH (in main resin) groups, as presented in Table 3.

Real-time rheological measurement of reactive clearcoats

The thermal curing behaviors of various clearcoat samples in Table 3 could be effectively characterized based on the real-time rheological properties [e.g., elastic (G') modulus] using a rotational rheometer (MCR-301, Anton Paar, Austria) equipped with a temperature-controllable convection-heating chamber.
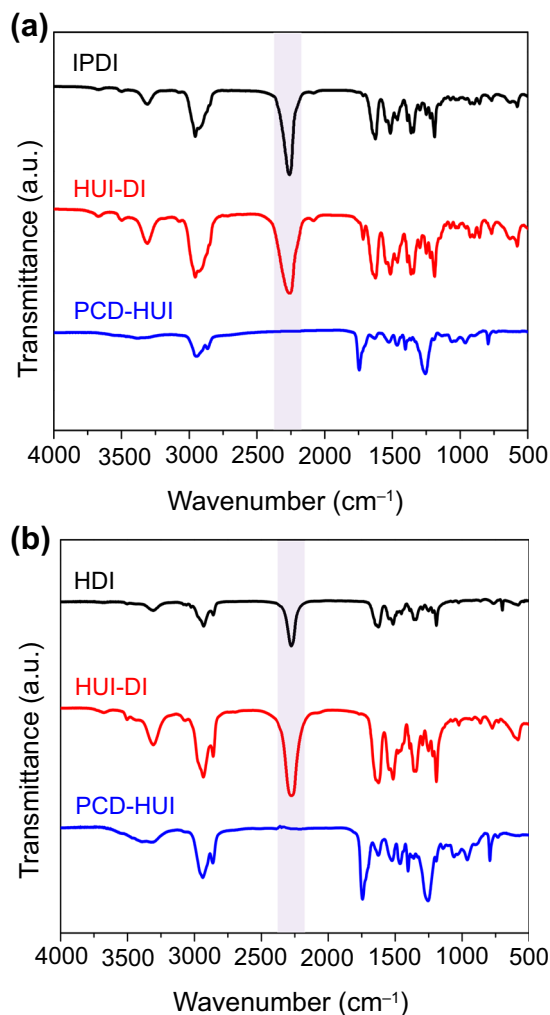
Table 1: Material and physical properties of PCD-HUI and PCD-HUH

	$\overline{M}_n$ (g/mol)	$\overline{M}_w$ (g/mol)	D_M	T_g (°C)	OH value (mg KOH/g)
PCD-HUI	2.5 k	5.5 k	2.20	−30.6	44.9
PCD-HUH	2.5 k	6.6 k	2.84	−44.5	40.0

Each clearcoat mixture was prepared using a vortex mixer (MX-S, Scilogex, USA) for 1 min before the test and maintained on the lower plate during the flash-off period of 5 min to sufficiently evaporate the volatile components. To simulate realistic thermal curing conditions, the measurement temperature was increased from 30 to 150°C at a heating rate of 10°C/min and maintained at 150°C for 20 min. The SAOS mode was employed to elucidate the real-time thermal crosslinking dynamics of the clearcoats, under a strain of 1% (of gap) and frequency of 1 Hz. A disposable plate with an 8 mm diameter was used in this test. During the measurement, the gap between the upper and lower plates was 300 μm.

Thermal properties of the clearcoat free films

The thermal properties of the cured clearcoat free films were evaluated by differential scanning calorimetry (DSC Q2000, TA Instruments, USA) and thermogravimetric analysis (TGA Q500, TA Instruments, USA). The glass transition temperatures (T_g) of the free films were determined using the first DSC heating ramp between 0 and 170°C at a rate of 10°C min^{-1} under a nitrogen atmosphere. The thermal degradation temperature (T_d) was measured by a TGA in the range of 25–600°C at a rate of 10°C min^{-1} under a nitrogen atmosphere to check the thermal stability at high temperatures. HI-30 exhibited a slightly higher T_g

Table 2: Formulation of reference clearcoats

Component	T30	T50
Acryl polyol	34.1	45.5
Polycarbonate diol	11.4	0
UV absorber	4	4
UV HALS	2	2
SWASOL 1500	23	23
Butyl acetate	20	20
Ethyl acetate	5.2	5.2
DBTDL	0.1	0.1
Leveling agent	0.2	0.2
Total	100	100

(43.5°C) than that of HH-30 (38.9°C) owing to its rigid ring structure. The T_d values of the two free films were found to be very similar (348.3°C for HI-30 and 349.5°C for HH-30).

DMA of the clearcoat free films

The thermomechanical properties of the cured clearcoat free films were measured using a DMA tester (DMA Q800, TA Instruments, USA). The rectangular cured films clamped in a film mode unit were vibrated at a frequency of 1 Hz and strain of 0.01% in the range of −80 to 140°C at a heating rate of 5°C min^{-1}.

Elastic recovery and scratch-healing properties of the clearcoat layers

Fabrication of the PCM sheet

To compare the elastic recovery and scratch-healing properties of the clearcoat layers in the PCM sheets for possible automotive coating applications, a phosphated metal steel (70 mm × 30 mm × 1 mm) was covered with a 20-μm-thick epoxy amine layer by electrical deposition. Waterborne primer and waterborne Blasé basecoat layers with thicknesses of 30 and 15 μm, respectively, were deposited in series using the conventional draw-down bar coating method and cured at 150°C for 30 min. Subsequently, the outmost clearcoat layer with a thickness of 40–50 μm was coated over the basecoat and cured at 150°C for 30 min.

Nano-indentation test

The elastic recovery characterization[31] of the PCM sheets was done using a nano-indentation tester (NHT[3], Anton Paar Tritec SA, Switzerland) with a diamond Berkovich-type indenter. The indentation properties, which are related to the viscoelastic recovery of the clearcoat layer in the PCM, were interpreted under the conditions of maximum force (e.g., 10 mN), loading–unloading rates (20 mN/min), and holding (pause) time (10 s).[32]

Table 3: OH values (OHV) and mixing ratios of clearcoats used in this study

Sample name	T50	T30	T50-PCD-HUI 10 wt%	T50-PCD-HUH 10 wt%	T50-PCD-HUI 30 wt%	T50-PCD-HUH 30 wt%
	R-1	R-2	HI-10	HH-10	HI-30	HH-30
OHV (mg KOH/g)	64.7	69.0	62.9	62.4	60.1	59.0
Resin/crosslinker[a]	3.21	3.01	3.31	3.33	3.46	3.52

[a]HDI-trimer NCO value = 207.9 mg/g, PCD-IPDI = 44.9 mg KOH/g, PCD-HDI = 40.0 mg KOH/g

Nano-scratch test

An NST (NST[3], Anton Paar Tritec SA, Switzerland) was employed to observe the quantitative changes in the scratches over the clearcoat layer in the PCM. A sphero-conical 90° indenter probe with a 2 μm radius was horizontally scanned over a length of 1 mm with a scratching speed of 2 mm/min on the coating surface with a progressive vertical load force (F_n). To measure the scratch penetration depth (P_d) and residual depth (R_d), the scratch tip under the progressive loading mode followed three procedures: (1) scanning of the initial profile of the coating surface with F_n of 0.1 mN, (2) linear increase in F_n along the scanned line up to the assigned maximum F_n for P_d, and (3) rescanning of the scratched surface with F_n of 0.1 mN for R_d.[33,34] In addition, an optical microscope (50 ×) was used to determine the first scratch fracture point (critical load, L_{c1})[25] based on the scratch profiles. In particular, the replicable healing feature of the scratches on the clearcoat layer in the PCM was elucidated by the repeated scratching and thermally driven healing procedures. Also, these scratching procedures were carried out using the progressive mode with a linear increase in the normal force along the same scratch trails.

Atomic force microscopy

The surface scratch-healing patterns after the scratch test conducted at constant normal force of 20 mN were characterized using AFM (AFM Wide Scan, Anton Paar Tritec SA, Switzerland) under various temperatures and durations.[35] The images were recorded with 256 scan lines for 256 s (i.e., single line scan per 1 s) in a total squared-scan area of 77.1 μm × 77.1 μm. The thermally driven scratch-healing patterns, temporally changing with the temperature (50 or 75°C) and time (until 12 h), were compared using 1D cross-cuts and 3D images. The 3D images were also utilized for the meticulous observation of the final (3rd) healed coating surface in the repeated scratch-healing operations on the same scratch positions.

Results and discussion

Real-time rheological properties of the clearcoats during the thermal curing

Real-time storage modulus data for the clearcoat samples were acquired using the rheometer during the thermal curing (Fig. 3). Under given heating conditions, they were crosslinked based on the urethane reaction between the hydroxyl group in the polyols and isocyanate functional group in the HDI trimer crosslinker. The different onset temperatures of the references and HH/HIs could be interpreted by the
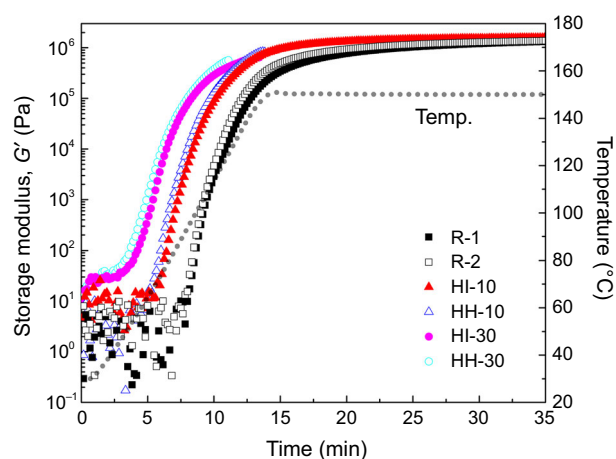

Fig. 3: Real-time rheological properties (G') of reactive clearcoat mixtures

different chemical reactivities of the primary and secondary hydroxyl groups. The clearcoat mixture consisted of a terminal-ended primary hydroxyl group in the PCD and side-branched secondary hydroxyl group in the acryl polyol. According to Ionescu,[36] a higher primary hydroxyl content in the clearcoat mixture leads to a higher overall reaction rate. Therefore, the clearcoat mixture containing the PCD-HU is expected to exhibit a rapid modulus growth under the same curing condition. The storage moduli of HI-30 and HH-30 began to increase immediately at the initial stage, while those of the references (R-1 and R-2) started to increase above 90°C. Although the initial curing reactions of the HI and HH series were faster than those of the references, the maximum storage moduli of the former were similar or slightly lower than those of the latter. Regardless of the content of PCD-HUI or PCD-HUH, the samples containing PCD-HUH had slightly faster curing times than those of the samples with PCD-HUI, considering the more flexible segmental motion of PCD-HUH with the linear structure.

Thermomechanical properties of the clearcoat free films

To produce clearcoat free films for DMA tests, the clearcoats were cured at 130°C for 1 h in a vacuum oven and left at room temperature for 3 days to completely evaporate the remaining solvents. Figure 4 shows the DMA results of the cured free films in the range of −80 to 140°C at a heating rate of 5°C min^{-1}. With the increase in measurement temperature, the elastic modulus begins to decrease from approximately 0°C, leading to peaks of tanδ in the range of 50–70°C. Compared to R-1, the tanδ-peak temperatures of the other samples decreased with the PCD content (including R-2, see Table 4), representing the more flexible crosslinked network structures. In general,
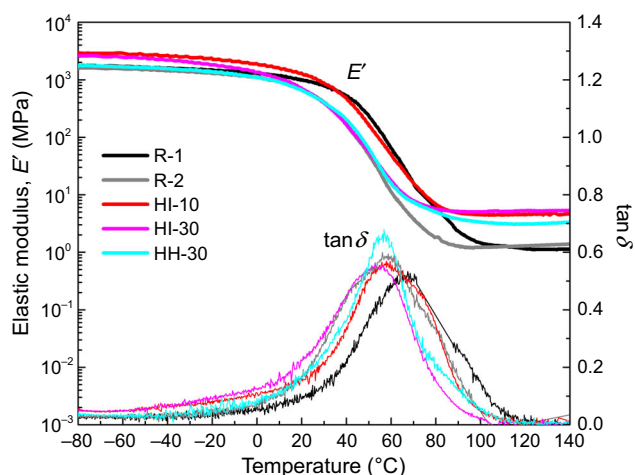
Fig. 4: DMA results of cured clearcoat free films

Table 4: Comparison of elastic moduli, T_g, and L_{c1} results for several clearcoat samples

	R-1	R-2	HI-30	HH-30
E' (MPa) (DMA at 30°C)	786.66	402.61	386.10	403.09
E' (MPa) (DMA at 140°C)	1.12	1.42	5.31	3.19
T_g (°C) (DMA)	67.47	56.03	52.92	56.76
L_{c1} (mN) (NST)	14.78	18.25	22.68	28.07

elastic moduli of free films containing the PCD-HUs were lower at room temperature but higher at 140°C (Table 4) in comparison with that of R-1 film, which might be closely related to scratch properties such as L_{c1}. This represents that the HU group in the PCD-HUs was in a more actively reversible state at high temperature, effectively reinforcing the modulus, because the bulky urea bond could be dissociated into isocyanate and amine and then could reversibly return to itself[37,38] under the heating.

Indentation and related elastic recovery properties of the cured clearcoat layers in the PCMs

The nano-indentation tests were carried out to measure the elastic recovery properties of the clearcoat layers in the PCM sheets. Figure 5a presents the indentation penetration depth (P_d)–normal force (F_n) curves on various clearcoat layers, confirming the strong effects of the amount and HU structure of the PCD-HUs on the indentation profiles. Despite the small normal force loading (10 mN), HH-30 was more flexible than the other samples. It could be deduced that HH-30 exhibited a considerably more flexible behavior in the scratch-healing, as will be explained later, owing to its high portion of HU groups and more flexible urethane network. Figure 5b shows the elastic

penetration depth recovered in the unloading stage (h_e), which stands for the elastic recovery property of the coating surface.[31] The maximum penetration depth could be thus divided into elastic and plastic deformation depths. Elastic portion is generally increased in the overall penetration depth, as the amount of PCD-HUs rises.

Scratch properties of the cured clearcoat layers in the PCMs

The intrinsic surface hardness values of the coating layers could be estimated using the scratch penetration depth (P_d) profiles upon the gradual load on the sphero-conical tip of 2 μm radius in the NST test. Figure 6a shows the scratch profiles including the scratch penetration (P_d) and residual (R_d) depths on the various coating layers under the progressive mode. The maximum normal force was set to 50 mN in this
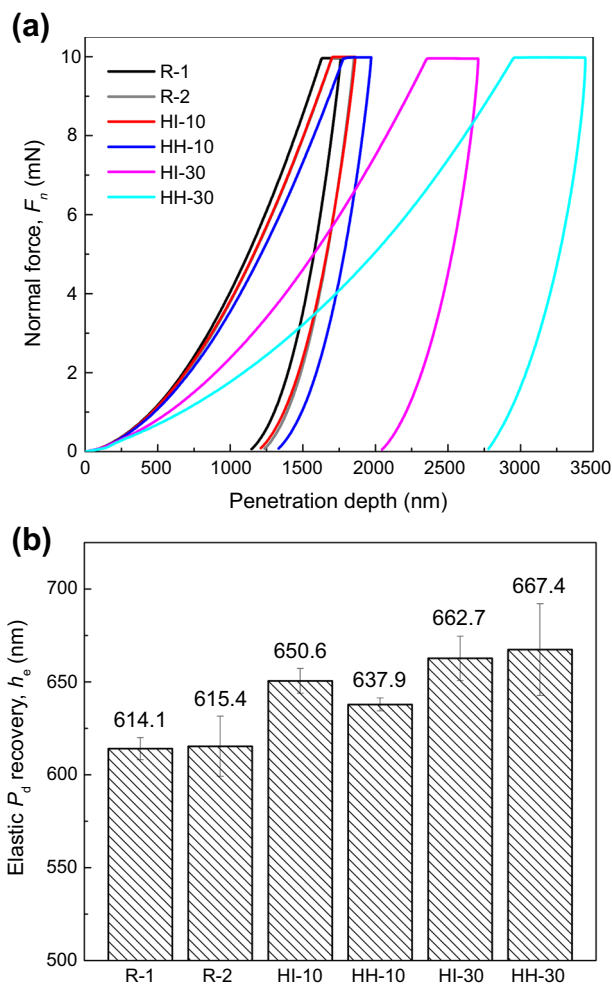

Fig. 5: Nano-indentation results of cured clearcoat layers. (a) P_d–F_n profiles and (b) the elastic penetration depth recovered at the final unloading
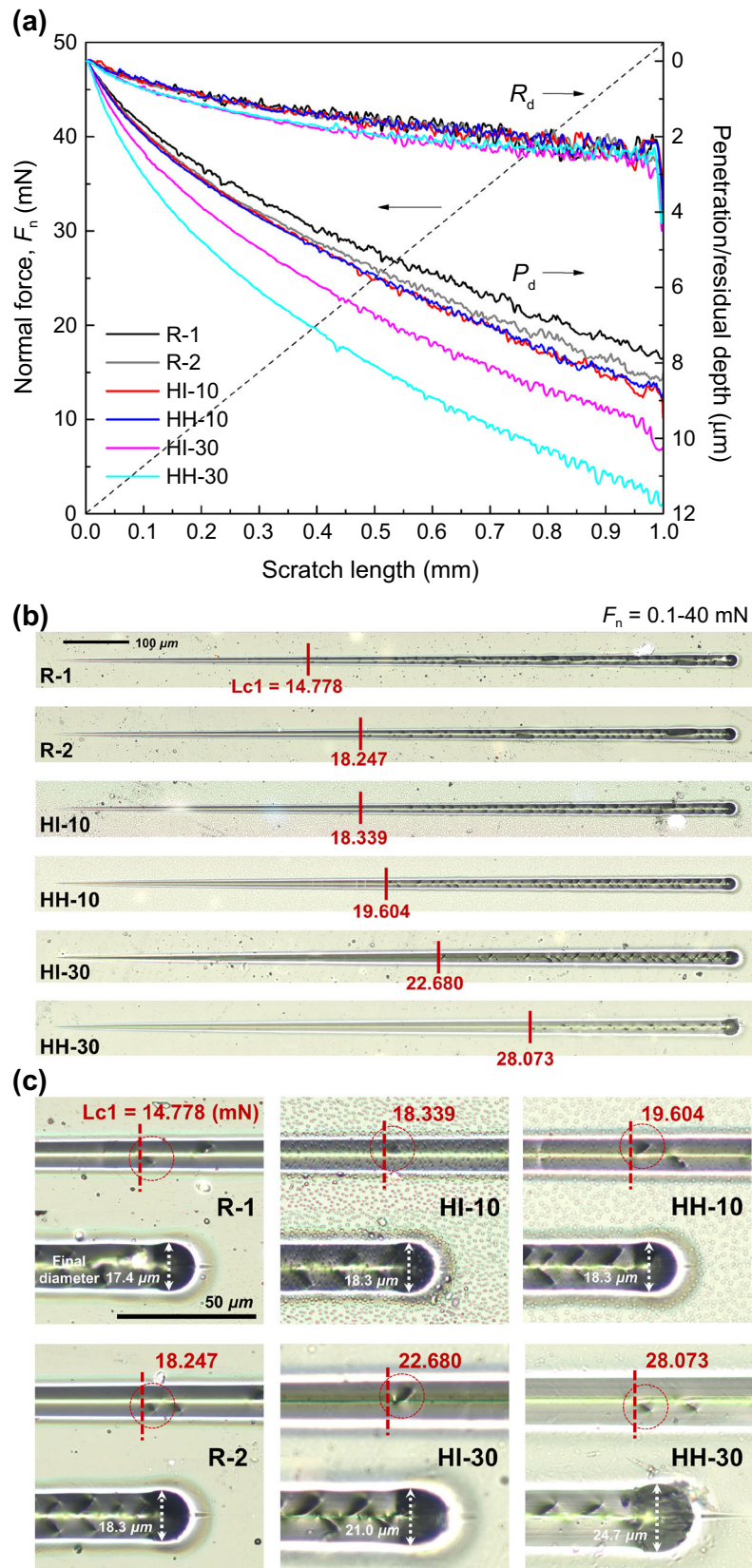
Fig. 6: Comparison of (a) scratch depth profiles of clearcoat layers and (b) their critical loads (L_{c1}) from optical images for residual depth profiles. (c) Enlarged images of (b) near L_{c1} and end regions

experiment to analyze in detail two scratch depths (P_d and R_d). R-1 exhibited the smallest P_d, followed by R-2. In the HI/HH series, those of HI-10 and HH-10 did not significantly differ. However, compared to that of HI-30, HH-30 with the slightly more flexible network generated a larger P_d, owing to the high PCD-HUH portion with the pliable linear structure.

In general, both urethane and urea groups in the PCD-HUs contribute to the formation of the flexible network,[36] considering their low T_g values, below –30°C (Table 1; note that the acryl polyol has T_g of approximately 50°C). A softer coating surface gives rise to a larger P_d at the same normal force load. This implies that the HI and HH series produced larger P_d values than those of the references. Despite the different P_d profiles of the various clearcoats, the residual R_d patterns were similar for all samples. Fast recoveries of the scratches in the HI-30 and HH-30 layers were observed due to their good elastic recovery properties. According to Vega et al.,[39] the healing of a scratched coating layer is divided into viscoelastic recovery (from P_d to R_d) and viscoplastic healing, which are thermally driven. Consequently, it is expected that a larger difference between R_d and P_d corresponds to a better recovery property. HH-30 offered the best scratch recovery, inversely related to the surface hardness. It is identified that HH-30 could show better scratch-healing properties through a proper thermal treatment than those of the other samples.

As depicted in Figs. 6b and 6c, the critical loads and final scratch shapes of the clearcoat layers were compared by observing their scratch patterns in the progressive mode via panoramic optical microscopic (50 ×) and enlarged images for residual depth profiles, respectively. The first scratch fracture points (critical load, L_{c1}) of the samples showed the same trend as the P_d patterns in Fig. 6a, indicating that the coatings with the relatively soft surfaces gave higher L_{c1} values. As displayed in Fig. 6c, the crack patterns were similar to each other, but at the end of the NST test, the scratch size (width) was found to increase slightly with the increase of the portion of PCD-HUs in clearcoats. These results also demonstrate that the PCD-HUs could more flexibly cope with these external stresses than the reference samples.

Scratch-healing pattern analysis by AFM

The transition of the scratch patterns engraved on the clearcoat layers was analyzed using 3D (Fig. 7) and 1D cross-cut (Fig. 8) images by AFM during the duration time at heated states (50 and 75°C). As shown in Figs. 7a and 7b, R-2 and HH-10 with initially similar surface properties displayed slightly different scratch-healing patterns at the same healing temperature and time (50°C for 12 h). In other words, R-2 and HH-10

had similar scratch patterns in the nano-scratch tests and the scratches on HH-10 were a little more remedied under given healing conditions, compared to those on R-2. Notably, HH-30 illustrated considerable changes (Fig. 7c) during the healing procedure; the peak and valley in its scratch quickly disappeared even after 1 h at 50°C, clearly reflecting the enhanced viscoelastic recovery and reversible attachment/detachment feature by the addition of PCD-HUs with urea group in clearcoats.

Figure 8 compares 1D cross-cut AFM images of the scratches on the clearcoat layers at the specific positions where the load of 20 mN was applied. The total scratch-healing rate based on the 1D cross-cut area was evaluated by equation (1), where R is the removal rate of scratched area, A_0 is the initial scratch cross-cut area, and A_x is the temporal scratch cross-cut area at the specified keeping time.

$$R = \frac{A_0 - A_x}{A_0} \times 100. \tag{1}$$

Figure 9 shows the removal rates of scratched area of the samples. At 50°C (Fig. 8a–8e), with the increase in keeping time, the scratches on all samples were steadily relaxed up to 12 h. For example, the scratch on HH-10 was healed to 62.8%, that on HI-10 to 50%, and that on R-2 to 47% after 12 h. Remarkably, HI-30 and HH-30 exhibited outstanding removal rates (96.4% for HH-30 and 94% for HI-30), owing to their flexible structures featured by the PCD-HUs. Note that the further increase in healing temperature (75°C) led to considerable changes in the scratches even at a heating time of 10 min (Fig. 8f). HI-10, HH-10, and R-2 had removal rates of scratched area of approximately 97% in this case. It can be concluded that the PCD-HUs in the coating system could provide enhanced scratch-healing performances under the given healing conditions.

Durability features through repeated scratching and healing procedures

The progressive-mode scratching (0.1–40 mN) and thermally driven healing (75°C, 12 h) procedures were repeated three times to investigate the durable abilities of the healed coating surfaces against the external stresses. The penetration and residual depth profiles of the scratches for R-2, HH-10, and HH-30 clearcoat layers during three-times scratch-healing procedures are portrayed in Fig. 10. The final healed scratch profiles (blue line) on the coating layers were obtained after the third scratching and subsequent healing. Even though the residual depth level was similar in each scratch stage, the fracture size in the residual scratch image steadily increased with the number of repeating cycles in the scratch test, implying that there exists a
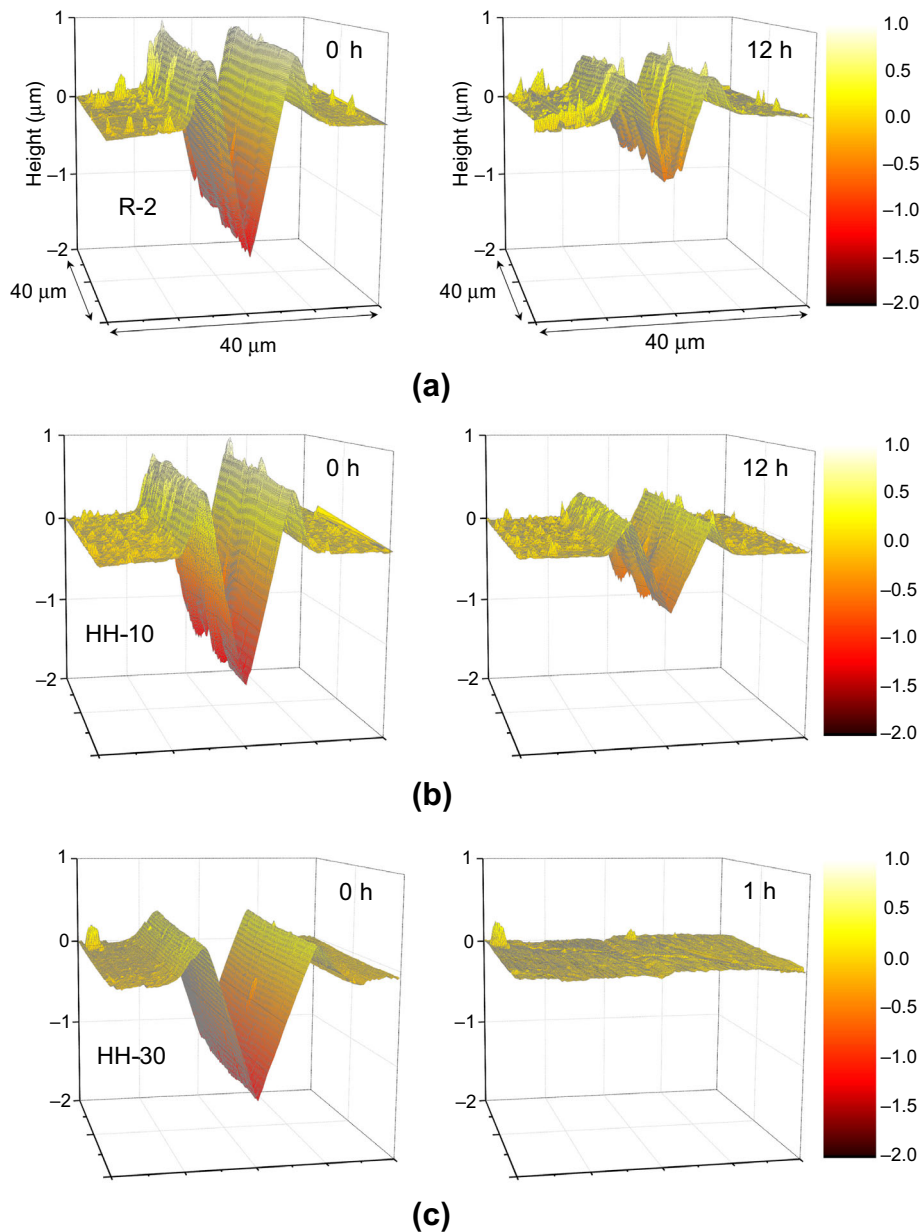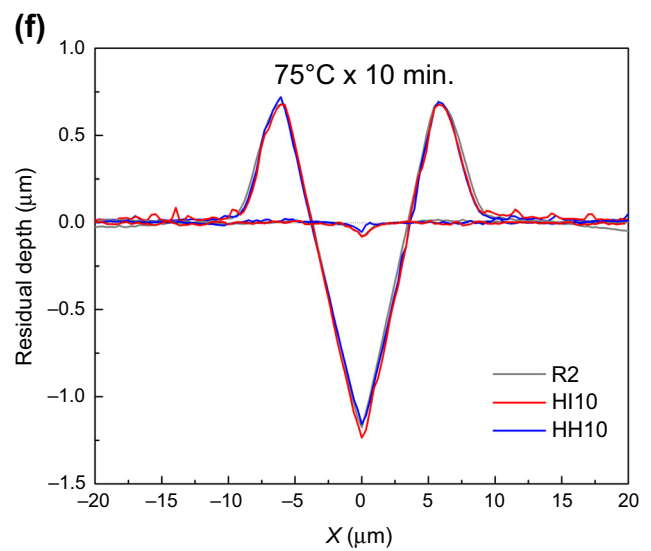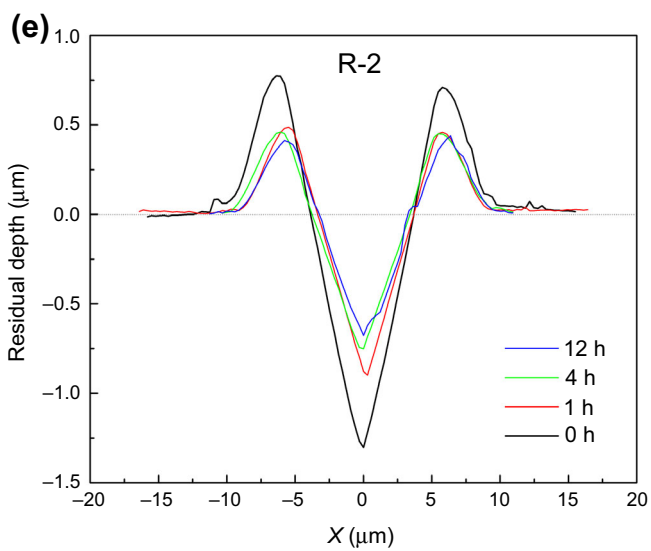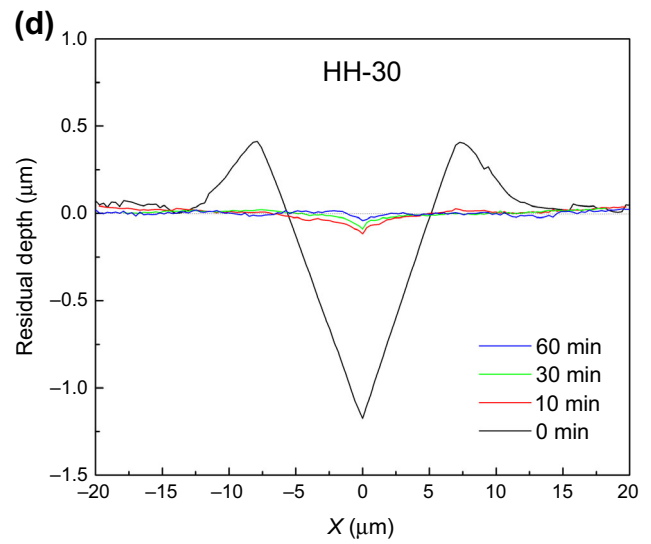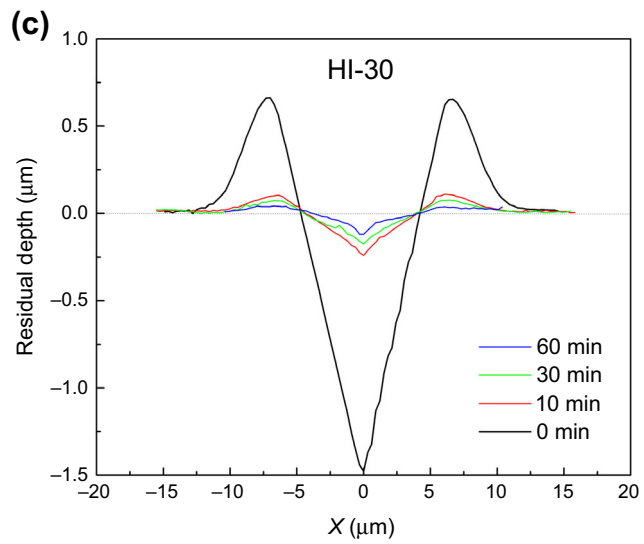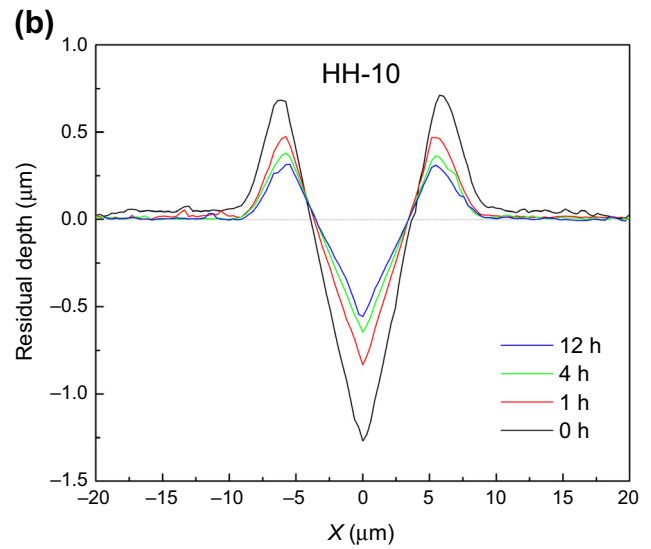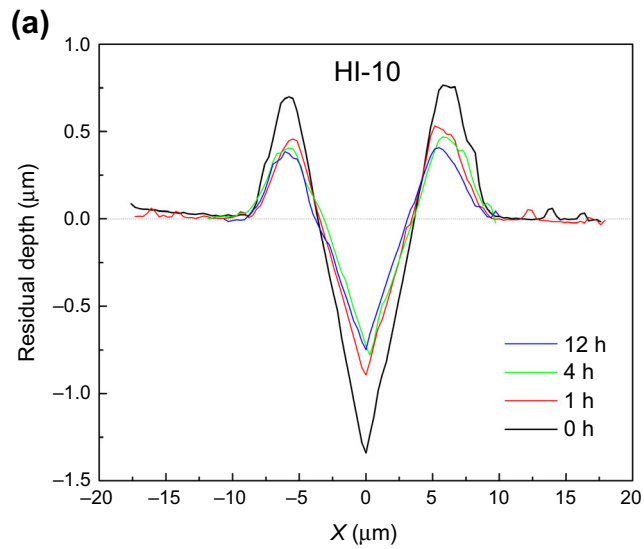
Fig. 7: Changes of 3D scratch patterns (at F_n = 20 mN) on several clearcoat layers under different duration times at 50°C for (a) R-2 (0 h and 12 h), (b) HH-10 (0 h and 12 h), and (c) HH-30 (0 h and 1 h)

little mass loss on scratched space during the repeated scratch-healing tests. Additionally, with the increase in the PCD-HU content, both fracture number and size considerably decreased due to its flexible feature and reversible exchange. Figure 11 shows panoramic images of the scratched surfaces for several clearcoat layers shown in Fig. 10 and their AFM 3D images at specific positions after the third scratch-healing test. The critical load point (L_{c1}) gradually decreased with the number of scratch test cycles. R-2 had a scratch fracture size of approximately 3 μm after the third

healing stage. The fracture effectively disappeared with the increase in the PCD-HU content. HH-30 had superior recovery and durability characteristics against perpetual external stresses.

Conclusions

The newly designed PCD-HUs for the 2 K clearcoats were systematically verified by rheological, thermal, and surface mechanical tests. Clearcoat mixtures with

(a)

(b)

(c)

(d)

(e)

(f)

◄Fig. 8: **Changes of 1D scratch patterns (at F_n = 20 mN) on several clearcoat layers under different duration times at 50°C for (a) HI-10, (b) HH-10, (c) HI-30, (d) HH-30, and (e) R-2. (f) Comparison of scratch patterns for several clearcoats for 10 min of 70°C**
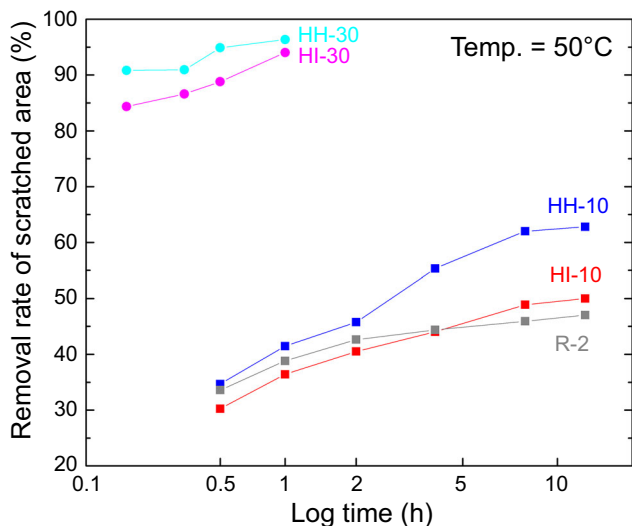

Fig. 9: **Removal rates of scratched area of various clearcoats**

the PCD-HUs (HI/HHs) exhibited similar or slightly lower maximum elastic moduli than those of the references but had lower curing onsets owing to their high reactivity in the real-time rheological measurement during the thermal curing. In addition, the HI/HH series bestowed thermomechanical properties favorable to scratch-healing at high temperature in the DMA test, compared to those of the references. Tests of the surface mechanical properties, including the nano-indentation and nano-scratch tests, clarified that HH-10 and R-2 with initially similar surface properties nevertheless showed different scratch shapes through the repeated scratching and thermally driven healing procedures. In addition, HI-30 and HH-30 exhibited better healing properties than those of the other samples at the same temperature and duration in the nano-indentation and single/repeated scratch tests. Results demonstrated that the clearcoat mixtures containing the PCD-HUs provided better scratch-healing characteristics at a given temperature and duration, capable of optimally tuning the healing properties as well as the rheological and surface mechanical properties of the clearcoat layers.
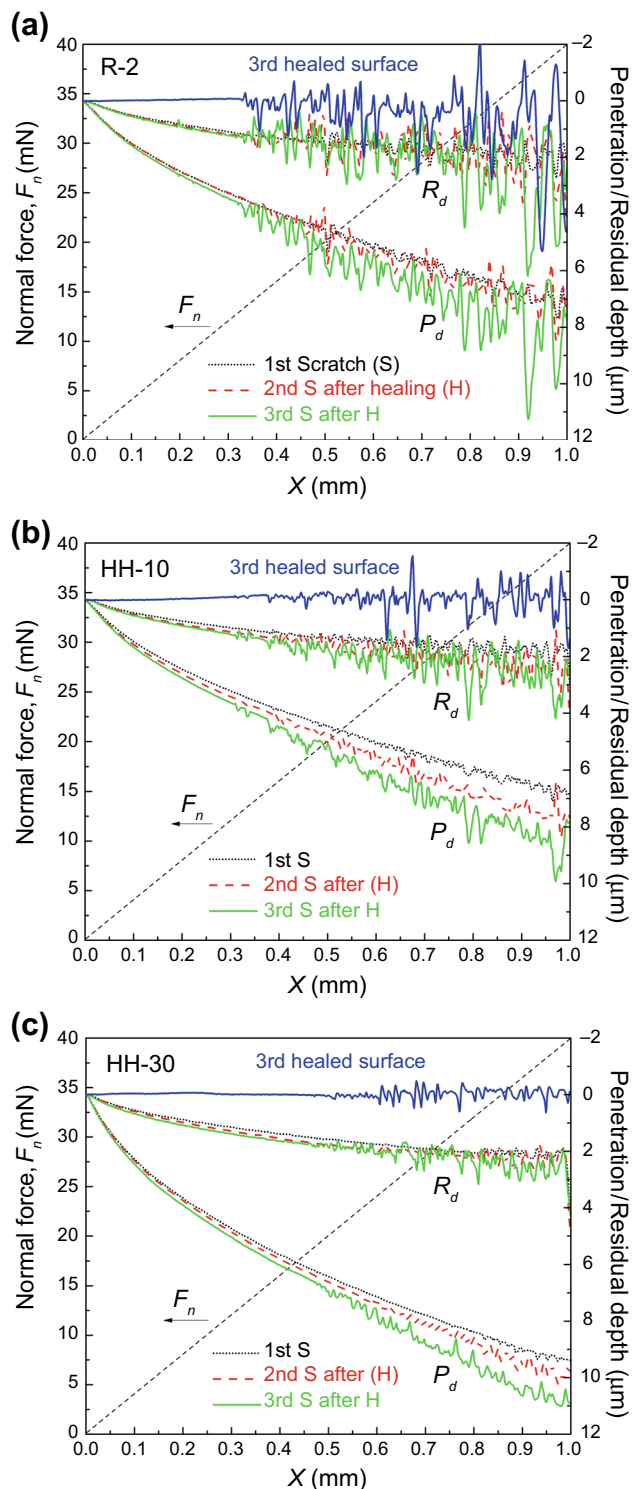

Fig. 10: **Scratch depth profiles of (a) R-2, (b) HH-10, and (c) HH-30 through repeated scratch-healing procedures**
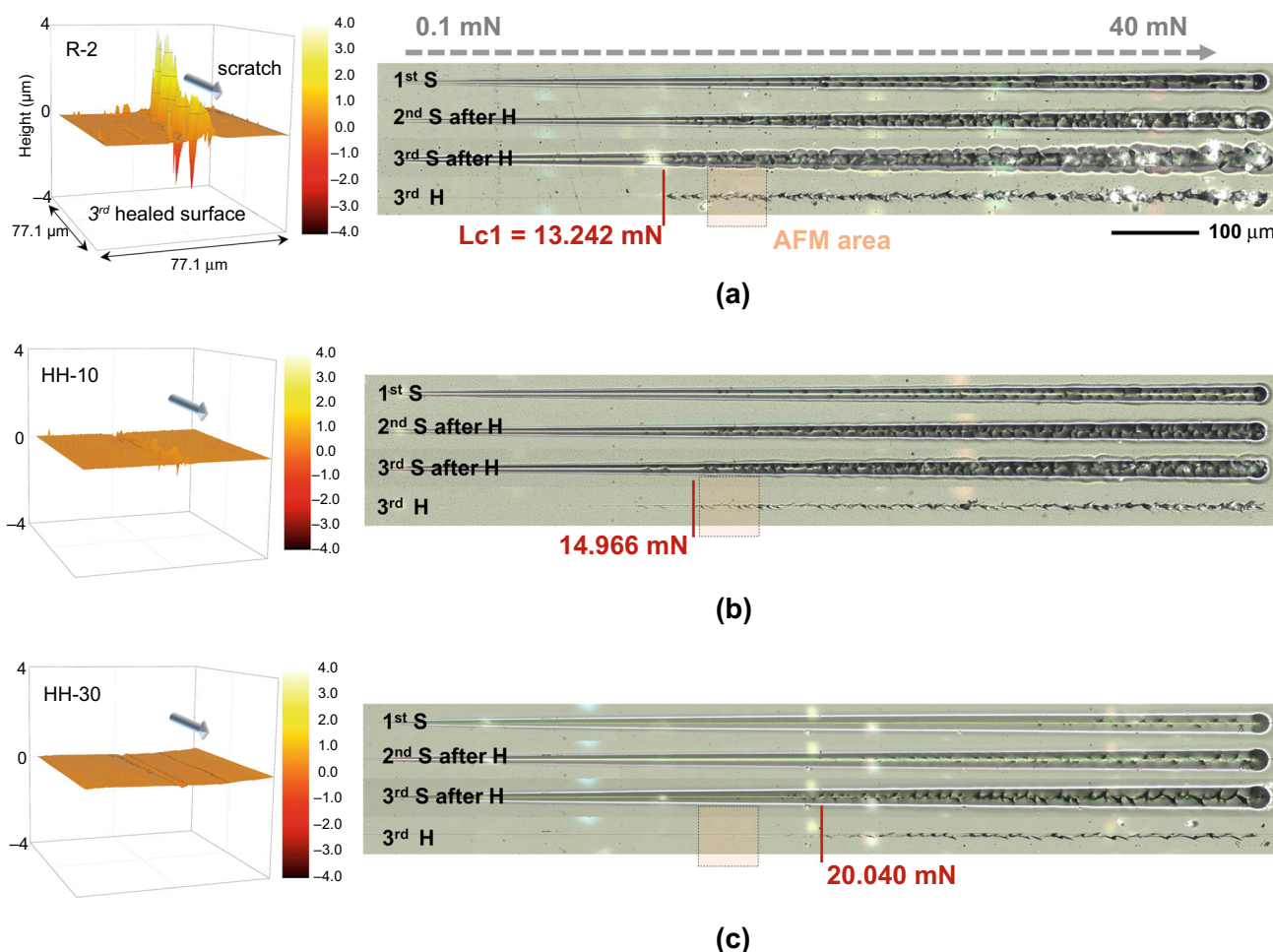
Fig. 11: Panoramic scratch views of (a) R-2, (b) HH-10, and (c) HH-30 clearcoats through repeated scratch-healing procedures and their AFM images after the third healing stage

References

1. Gregorovich, B, Hazan, I, "Environmental Etch Performance, and Scratch and Mar of Automotive Clearcoats." *Prog. Org. Coat.*, **24** 131–146 (1994)
2. Lange, J, Luisier, A, Hult, A, "Influence of Crosslink Density, Glass Transition Temperature and Addition of Pigment and Wax on the Scratch Resistance of an Epoxy Coating." *J. Coat. Technol.*, **69** 77–82 (1997)
3. Kotnarowska, D, Wojtyniak, M, "Nanotechnology Application to Automotive Coating Manufacturing." *J. KONES*, **14** 253–258 (2007)
4. Tahmassebi, N, Moradian, S, Ramezanzadeh, B, Khosravi, A, Behdad, S, "Effect of Addition of Hydrophobic Nano Silica on Viscoelastic Properties and Scratch Resistance of an Acrylic/Melamine Automotive Clearcoat." *Tribol. Int.*, **43** 685–693 (2010)
5. Scrinzi, E, Rossi, S, Kamarchik, P, Deflorian, F, "Evaluation of Durability of Nano-Silica Containing Clear Coats for Automotive Applications." *Prog. Org. Coat.*, **71** 384–390 (2011)
6. Lee, DG, An, SY, Um, MS, Choi, WJ, Noh, SM, Jung, HW, Oh, JK, "Photo-Induced Thiol-Ene Crosslinked Polymethacrylate Networks Reinforced with Al_2O_3 Nanoparticles." *Polymer*, **101** 119–126 (2016)
7. Ramezanzadeh, B, Moradian, S, Tahmasebi, N, Khosravi, A, "Studying the Role of Polysiloxane Additives and Nano-SiO_2 on the Mechanical Properties of a Typical Acrylic/Melamine Clearcoat." *Prog. Org. Coat.*, **72** 621–631 (2011)
8. Streitberger, H, Dossel, K, *Automotive Paints and Coatings.* WILEY-VCH, Weinheim (2008)
9. Urban, M, Allison, C, Finch, C, Tatro, B, "Interfacial Studies of Crosslinked Urethanes: Part III. Structure–Property Relationships in Polyester Waterborne Polyurethanes." *J. Coat. Technol.*, **71** 75–85 (1999)
10. Bertrand-Lambotte, P, Loubet, J, Verpy, C, Pavan, S, "Nano-Indentation, Scratching and Atomic Force Microscopy for Evaluating the Mar Resistance of Automotive Clearcoats: Study of the Ductile Scratches." *Thin Solid Films*, **398** 306–312 (2001)

11. Blaiszik, BJ, Kramer, SL, Olugebefola, SC, Moore, JS, Sottos, NR, White, SR, "Self-Healing Polymers and Composites." *Ann. Rev. Mater. Res.*, **40** 179–211 (2010)
12. Yoon, JA, Kamada, J, Koynov, K, Mohin, J, Nicolaÿ, R, Zhang, Y, Balazs, AC, Kowalewski, T, Matyjaszewski, K, "Self-Healing Polymer Films Based on Thiol–Disulfide Exchange Reactions and Self-Healing Kinetics Measured Using Atomic Force Microscopy." *Macromolecules*, **45** 142–149 (2011)
13. AbdolahZadeh, M, Esteves, A, Van der Zwaag, S, Garcia Espallargas, S, "On the Healing Mechanism of Sol–Gel Derived Hybrid Materials Containing Dynamic Di-Sulfide Bonds," ICSHM 2013: Proceedings of the 4th International Conference on Self-Healing Materials, Ghent, Belgium (2013)
14. Yarmohammadi, M, Shahidzadeh, M, Ramezanzadeh, B, "Designing an Elastomeric Polyurethane Coating with Enhanced Mechanical and Self-Healing Properties: The Influence of Disulfide Chain Extender." *Prog. Org. Coat.*, **121** 45–52 (2018)
15. Gao, F, Cao, J, Wang, Q, Liu, R, Zhang, S, Liu, J, Liu, X, "Properties of UV-Cured Self-Healing Coatings Prepared with PCDL-Based Polyurethane Containing Multiple H-Bonds." *Prog. Org. Coat.*, **113** 160–167 (2017)
16. Grzelak, AW, Boinard, P, Liggat, JJ, "The Influence of Diol Chain Extender on Morphology and Properties of Thermally-Triggered UV-Stable Self-Healing Polyurethane Coatings." *Prog. Org. Coat.*, **122** 1–9 (2018)
17. Liu, YL, Chuo, TW, "Self-Healing Polymers Based on Thermally Reversible Diels–Alder Chemistry." *Polym. Chem.*, **4** 2194–2205 (2013)
18. Kim, SY, Lee, TH, Park, YI, Nam, JH, Noh, SM, Cheong, IW, Kim, JC, "Influence of Material Properties on Scratch-Healing Performance of Polyacrylate-Graft-Polyurethane Network that Undergo Thermally Reversible Crosslinking." *Polymer*, **128** 135–146 (2017)
19. Sung, S, Kim, SY, Lee, TH, Favaro, G, Park, YI, Lee, SH, Ahn, JB, Noh, SM, Kim, JC, "Thermally Reversible Polymer Networks for Scratch Resistance and Scratch Healing in Automotive Clear Coats." *Prog. Org. Coat.*, **127** 37–44 (2019)
20. Zechel, S, Geitner, R, Abend, M, Siegmann, M, Enke, M, Kuhl, N, Klein, M, Vitz, J, Gräfe, S, Dietzek, B, "Intrinsic Self-Healing Polymers with a High *E*-Modulus Based on Dynamic Reversible Urea Bonds." *NPG Asia Mater.*, **9** e420 (2017)
21. Ying, H, Zhang, Y, Cheng, J, "Dynamic Urea Bond for the Design of Reversible and Self-Healing Polymers." *Nat. Commun.*, **5** 3218 (2014)
22. Lin, L, Blackman, G, Matheson, R, "A New Approach to Characterize Scratch and Mar Resistance of Automotive Coatings." *Prog. Org. Coat.*, **40** 85–91 (2000)
23. Bertrand-Lambotte, P, Loubet, J, Verpy, C, Pavan, S, "Understanding of Automotive Clearcoats Scratch Resistance." *Thin Solid Films*, **420** 281–286 (2002)
24. Shen, W, Mi, L, Jiang, B, "Characterization of Mar/Scratch Resistance of Coatings with a Nano-Indenter and a Scanning Probe Microscope." *Tribol. Int.*, **39** 146–158 (2006)
25. Noh, SM, Lee, JW, Nam, JH, Park, JM, Jung, HW, "Analysis of Scratch Characteristics of Automotive Clearcoats Containing Silane Modified Blocked Isocyanates via Carwash and Nano-Scratch Tests." *Prog. Org. Coat.*, **74** 192–203 (2012)
26. Noh, SM, Nam, JH, Oh, JK, Jung, HW, "Scratch and Recovery Characteristics of Automotive Clearcoats Containing Blocked Polyisocyanate Crosslinkers." *J. Coat. Technol. Res.*, **12** 85–95 (2015)
27. Kutschera, M, Sander, R, Herrmann, P, Weckenmann, U, Poppe, A, "Scratch Resistance of Automobile Clearcoats: Chemistry and Characterization on the Micro-and Nanoscale." *J. Coat. Technol. Res.*, **3** 91–97 (2006)
28. Shen, WC, Jiang, B, Jones, FN, "Measurement of Mar Resistance and Study of Marring Mechanism of Polymeric Coatings with Scanning Probe Microscope." *J. Coat. Technol.*, **72** 89–95 (2000)
29. Seubert, C, Nichols, M, Henderson, K, Mechtel, M, Klimmasch, T, Pohl, T, "The Effect of Weathering and Thermal Treatment on the Scratch Recovery Characteristics of Clearcoats." *J. Coat. Technol. Res.*, **7** 159–166 (2010)
30. Park, JI, Choe, A, Kim, MP, Ko, H, Lee, TH, Noh, SM, Kim, JC, Cheong, IW, "Water-Adaptive and Repeatable Self-Healing Polymers Bearing Bulky Urea Bonds." *Polym. Chem.*, **9** 11–19 (2018)
31. Feng, ZQ, He, QC, Zeng, Q, Joli, P, "Theory of Nanoindentation, Chapter 26." In: Sattler, KD (ed.) *Handbook of Nanophysics: Functional Nanomaterials*. CRC Press, Boca Raton (2010)
32. Jung, KI, Hwang, SO, Kim, NH, Lee, DG, Lee, JH, Jung, HW, "Effect of Methacryloxypropyl and Phenyl Functional Groups on Crosslinking and Rheological and Mechanical Properties of Ladder-Like Polysilsesquioxane Hard Coatings." *Prog. Org. Coat.*, **124** 129–136 (2018)
33. ASTM D7187-15, Standard Test Method for Measuring Mechanistic Aspects of Scratch/Mar Behavior of Paint Coatings by Nanoscratching (2015)
34. Feng, L, Benhamida, BN, Lu, CY, Sung, LP, Morel, P, Detwiler, AT, Skelly, JM, Baker, LT, Bhattacharya, D, "Fundamentals and Characterizations of Scratch Resistance on Automotive Clearcoats." *Prog. Org. Coat.*, **125** 339–347 (2018)
35. Scheltjens, G, Diaz, M, Brancart, J, Van Assche, G, Van Mele, B, "A Self-Healing Polymer Network Based on Reversible Covalent Bonding." *React. Funct. Polym.*, **73** 413–420 (2013)
36. Ionescu, M, *Chemistry and Technology of Polyols for Polyurethanes*. Smithers Rapra Publishing, Shrewsbury (2005)
37. Stowell, JC, Padegimas, SJ, "Urea Dissociation. Measure of Steric Hindrance in Secondary Amines." *J. Organ. Chem.*, **39** 2448–2449 (1974)
38. Hutchby, M, Houlden, CE, Ford, JG, Tyler, SN, Gagné, MR, Lloyd-Jones, GC, Booker-Milburn, KI, "Hindered Ureas as Masked Isocyanates: Facile Carbamoylation of Nucleophiles Under Neutral Conditions." *Angew. Chem. Int. Edit.*, **48** 8721–8724 (2009)
39. Vega, J, Grande, A, Van der Zwaag, S, Garcia, S, "On the Role of Free Carboxylic Groups and Cluster Conformation on the Surface Scratch Healing Behaviour of Ionomers." *Eur. Polym. J.*, **57** 121–126 (2014)